This document contains the draft version of the following paper:

W. Bejgerowski, S.K. Gupta, and H.A. Bruck, "A systematic approach for designing multi-functional thermally conducting polymer structures with embedded actuators," *ASME Journal of Mechanical Design*, 131 (11): 111009, 2009.

Readers are encouraged to get the official version from the journal's website or by contacting Dr. S.K. Gupta (skgupta@umd.edu).

A Systematic Approach for Designing Multi-Functional Thermally Conducting Polymer Structures with Embedded Actuators

Wojciech Bejgerowski, Satyandra K. Gupta[1] and Hugh A. Bruck*

Department of Mechanical Engineering, University of Maryland, College Park, MD 20742
*Institute for Systems Research, University of Maryland, College Park, MD 20742

Abstract

Thermally conductive filled polymers enable the creation of multi-functional structures that offer both anchoring points for the embedded actuators as well as heat dissipation functions in order to facilitate the miniaturization of devices. However, there are two important challenges in creating these structures: (1) sufficient thermal management to prevent failure of the actuator, and (2) the ability of the actuator to survive the manufacturing process. This paper describes a systematic approach for design of multi-functional structures with embedded heat generating components using an in-mold assembly process to address these challenges. For the first challenge, development of appropriate thermal models is presented along with incorporation of in-mold assembly process constraints in the optimization process. For the second challenge, a simulation of the molding process is presented and demonstrated to enable determination of processing conditions ensuring survival of the in-mold assembly process for the embedded actuator. Thus, the design methodology described in this paper was utilized to concurrently optimize the choice of material, size of the structure and processing conditions in order to demonstrate the feasibility of creating multi-functional structures from thermally conductive polymers by embedding actuators through an in-mold assembly process.

1 Introduction

Miniaturization is gaining interest in many applications, where size and weight play an important constraint. Some of these applications include hard disks, cameras, cell phones, micro air vehicles, medical robots, and drug delivery systems. In-mold assembly using conventional manufacturing processes like injection molding can improve the miniaturization process by overcoming manufacturing limitations related to the challenges of integrating small functional components, such as actuators, into miniaturized polymeric structures by eliminating the manual assembly operation [1]. This however poses two important challenges. The first is thermal management, since embedded actuators generate heat during operation that must be dissipated. If the heat dissipation is not sufficient, the heat generated by actuators will increase the temperature at the interface between the embedded actuator and anchoring polymer structure causing either (a) the polymer at the interface to melt resulting in failure of the anchoring point for the actuator or (b) overheating of the actuator, both of which will lead to subsequent dysfunction of the actuator. Therefore a "multi-functional" structure is required, which will serve as a structural housing and also as the heat sink for the embedded actuator. The second important challenge is the ability for the actuators to survive the in-mold assembly process. Injection of a polymer melt into a mold cavity under high pressure has the potential for destroying delicate features of the actuators before they are fully embedded, which may prevent proper functioning of the actuator.

Several researchers have previously reported embedding actuators in polymers for robotic structures. However, they do not discuss the thermal challenges due to the use of polymers as the structure material, required from the injection molding point of view. Kim and Tadokoro [1] present modeling, analysis and control method of a prestrained dielectric elastomer actuator being embedded in a segment of an ANTLA inchworm microrobot. Three ANTLAs embedded in the metameric structure of the robot provide 3 DOF actuation. They present a prototype capable of translational motion, however the scale and actuation method is mainly targeted at a morphological structure similar to an annelid. Rosmarin and Asada [2] developed a humanoid hand with hybrid DC motor–SMA actuator arrays embedded in the palm. ABS fingers are actuated by a series of pulleys driven from the palm, which is composed of steel plates. The authors mention

[1] Corresponding Author

using cooling fans, which suggests that even though the SMA wires are not directly embedded in the polymer structure, there is a need for active cooling.

We will use miniature robots to illustrate the problems associated with thermal management of heat generated by embedded actuators. For example, insufficient dissipation of heat generated by embedded actuators has been observed in miniature robotic devices, such as the Minimally Invasive Neurosurgical Intracranial Robot (MINIR) [3] or flapping wing micro-air vehicle (MAV) [4]. The MINIR, developed in the RAMS Lab, was assembled from Delrin machined parts and SMA wires threaded through them. Due to the absence of active cooling or adequate passive heat dissipation, the embedded SMA wire actuators heated up the anchoring polymer structure during operation, causing the anchoring polymer structure to reach its softening temperature which resulted in loss of load transfer to the structure. In the MAV application, a DC motor used as an actuator was placed in an ABS mechanism frame. This actuator was cooled in-flight by the air flowing over it, and hence functionality was maintained. However, overheating was observed while testing the MAV in a fixed stand over the long periods of time due to reduced air flow.

In many small scale applications the utilization of heat sinks commonly used at the macroscale is not a viable option due to reduced weight and size budget. Using an active cooling method may also not be an acceptable option due to the additional power consumption, weight and complexity it introduces. Filled polymer composites are already gaining interest by researchers in many areas [5-6]. Since thermally conductive filled polymers are promising for the heat dissipation function, their thermal behavior needs to be characterized when using them for the embedding of actuators. Many injection-moldable filled polymers currently available on the market have thermal conductivities which are an order of magnitude higher then bulk unfilled polymers (see Table 1). Using these materials allows for creating multi-functional structures that offer both anchoring points for actuators, as well as heat dissipation function. Several researchers have studied the thermal performance of these materials, however they have not investigated the possibility of their application to in-mold assembly process.

Weber et al. [7] observed synergistic effect of combining different carbon fillers on thermal conductivity of carbon filled nylon 6,6 and polycarbonate based resins. The three carbon fillers investigated included an electrically conductive carbon black, synthetic graphite particles, and a milled pitch-based carbon fiber. They determined the effects and interactions of each filler on the thermal conductivity properties of the conductive resins.

Bahadur and Bar-Cohen [8] investigated the thermal performance limits of a polyphenylene sulphide polymer composite pin fin heat sinks cooled with air. They analytically predicted the thermal performance across an extensive parametric space in terms of the primary thermal metrics and identified the thermal performance limits. They showed that PPS heat sinks are a viable alternative material for energy efficient heat sink design with thermal performance comparable to aluminum and copper heat sinks at low fin densities and pumping power.

Bahadur [9] also presented thermal simulations and measurements with application to heat sink design fabricated out of thermally conductive polymer composites. He presents theoretical models and validation techniques to predict and optimize the filler orientation for the heat dissipation function, however this work is addressing only pin pins heat sink designs.

Dogruoz et al [10] studied thermal performances of advanced heat sink materials via computational models, and compared them with Aluminum heat sinks. They presented transfer functions based on the heat sink geometry, material properties (thermal conductivity) and the base temperature.

Egelkraut et al. [11] demonstrated the potential of highly filled polymers for packaging solutions in power electronics and present a packaging technology for passive devices. They used a choke for a high power multiphase DC/DC converter packaged in a highly filled thermal conductive thermo-plastic polymer using an injection molding process. Based on thermal simulations, polymers with different Al_2O_3 filler volume fractions were produced and used as housing. The high filler volume fraction and the thermal conductivity led to changes in process conditions, especially with respect to temperature and pressure during the molding process.

This paper introduces a design methodology for filled polymer structures with embedded heat-generating actuators using an in-mold assembly process, taking into account the processing conditions. The thermal behavior of thermally conductive filled polymers is characterized and modeled for the in-mold assembly process. Both thermal and processing models are developed for predicting thermal management and survivability of the embedded actuator respectively using commonly available software packages. Experiments are designed and performed using resistors as surrogate heat generating elements to calibrate the models. Both unfilled Polyamide 12 and a PA 12-based thermally conductive filled polymer were used in order to determine the difference in operating temperature for unfilled and filled structures. The thermal models are then used to investigate the sensitivity of the filler orientation resulting from the in-mold assembly process to the heat dissipation function. Experiments were then conducted to determine if the thermal properties of the thermally conductive filled polymers are sufficient to run embedded actuators at an acceptable temperature that ensures

both structural and thermal functionality. Finally, the processing model is used to determine processing conditions ensuring motor survivability during in-mold assembly, and then experiments are conducted to demonstrate feasibility of creating multi-functional structures from thermally conductive polymers by embedding actuators through an in-mold assembly process.

2 Overview of the Design Process

This section describes the overall approach for designing structures with embedded actuators to be manufactured using in-mold assembly process. The goal of the approach is to concurrently optimize the choice of material, size of the structure and processing conditions. The objective function of this optimization is to minimize the weight for miniaturization of robotic devices, but it can be also chosen to be compatible with any other design requirements. In order to perform this optimization process, first a selection of moldable material needs to be made for ensuring the thermal performance. Next, the appropriate thermal model of the structure needs to be developed to asses if the heat from the actuator is dissipated sufficiently through the filled polymer structure. The actuator to be embedded imposes certain constraints due to its strength to eliminate the possibility of damaging the actuator due to forces exerted by the manufacturing process. Finally, the geometry of the structure and in-mold assembly processing conditions needs to be parameterized. The overall general approach is outlined in Fig. 1.

The development of thermal model of the structure with embedded actuator is usually not straight forward due to various parameters that need to be considered. Thermal conductivity of injection-moldable polymers is enhanced by adding conductive fillers (usually carbon microfibers) to the polymer. These fillers tend to get aligned with the polymer flow during injection into the mold, resulting in non-isotropic thermal and mechanical properties. These properties can be controlled through careful gate positioning in the mold to control fiber orientation during flow of the polymer melt. Accurate modeling of thermal properties resulting from the fiber orientation is a very complicated task. However, for the heat dissipation capability assessment, the tedious orthotropic modeling may not be required once a material with sufficient thermal conductivity is chosen, since only sufficient heat transfer path is required from the design point of view. Nevertheless, the actual value of thermal conductivity has to be chosen with care. Also, establishing the natural free convection coefficient for the thermal model is not obvious, as it depends on both material characteristics and the geometry. Section 3 of this paper presents a systematic approach of determining these thermal modeling variables with sufficient accuracy for the heat dissipation task.

After developing the appropriate thermal model, the structure geometry and process parameters need to be parameterized for the optimization procedure. Depending on the functional requirements of the designed part the design variables and parameters have to be chosen appropriately. These will include the parameterized geometry of the structure as well processing conditions. The mold used for in-mold assembly, in addition to all regular mold designing rules, needs to be designed in a way to allow for fixating actuators in order for them to be embedded correctly. This also requires securing heat sensitive features of the actuators from the hot polymer melt. The actuator to be embedded will also pose certain constraints on the process parameters. The injection temperature and pressure are the most important parameters to be controlled, ensuring both proper filling of the mold and survivability of the embedded actuator. The temperature of the polymer melt has to be chosen correctly, so that the viscosity of the melt will be sufficient to fill the mold cavity. At the same time, it can not thermally shock the embedded component. The injection pressure has to be also chosen correctly to allow for filling of the entire mold cavity and ensure that the embedded component will not experience plastic deformation over the acceptable limit. Therefore the actuator constraints on the process parameters need to be incorporated to the parametric optimization to ensure functionality of the final product, which will be discussed in Section 4 of this paper.

3 Development of Thermal Model

From the application point of view, it is desirable to use thermal Finite Element Analysis (FEA) to predict heat dissipation from embedded actuators, and hence be able to assess their proper functionality in miniature devices on the design level. Since thermal modeling of embedded electronic components is a research area on its own [11-14], the experimental data was used to verify and calibrate the modeling approach. Also, because of the complexity of modeling a real actuator, a resistor was first used as a surrogate with similar heat generation and geometric characteristics. This was followed by a more complex motor assembly model discussed in Section 4 to test the versatility of the modeling approach.

3.1 Acquiring Experimental Data for Model Calibration

A heat dissipation experiment was designed and performed to verify and calibrate the thermal FEA modeling approach for a structure with an embedded electronic element as a heat source. For sample preparation, Grilamid L16 Natural from EMS-Chemie was used as the bulk polyamide material and thermally conductive NJ-6000 TC polyamide compound from PolyOne as the filled polymer. Hence, it was possible to quantify and justify the difference made by using thermally conductive polymers to dissipate heat from embedded actuators. The main physical properties of the materials are listed in Table 1.

A 1 Watt, 1 k-Ohm metal-oxide resistor from Radio Shack was used as the electronic component producing heat during operation. The resistor was placed in the center of the cylindrical cavity of the mold. Precision-milled cavities on the parting surface of both mold halves ensured adequate clamping, and hence accurate positioning of the resistor. A thermocouple was also placed in the mold cavity to allow for experimental verification of the modeling approach by direct temperature measurement of the embedded resistor. The thermocouple was supplied through a hole in the back of the mold, opposite to the sprue/gate. The mold assembly is shown in Fig. 2. Distance disks were used to overcome mold filling difficulties. A Babyplast injection molding machine was used to assemble the samples in-mold during injection. The resistivity of the resistor was measured before and after embedding with a Fluke 87 True RMS Multimeter and determined to be within 8% from the nominal value, thereby verifying that no damage occurred during the in-mold assembly process.

In order to control the amount of heat generated, the embedded resistors were connected to a HP Harrison 6205B Power Supply at 31.62 V. The amount of heat generation was verified by direct measurement of the current in the resistor circuit. The temperatures were recorded by Omega® HH506R Thermometer, which transferred the data to a PC through a RS-232 port. Using Omega® IV Recording Software, it was possible to automatically measure two temperatures for extended periods of time. This, along with shielding of the experimental setup, ensured the steady-state natural convection conditions. First, the ambient temperature was recorded along with temperatures in different points on the surface of the cylinder. In the second setup, the ambient temperature was measured along with the embedded thermocouple reading. All thermocouples used in the experiment were Omega® 5TC-GG-K-20-36. Table 2 contains the dimensions of prepared samples. A schematic of sampling points is shown in Fig. 3. However, sectioning of in-mold assembled samples showed that the embedded thermocouple may not necessarily be in contact with the resistor, which will be further discussed in Section 3.3.

3.2 Thermal Model Description

The thermal FEA model of the samples described in Section 3.1 was developed using SolidWorks 2007 software. The model consists of an assembly of resistor and polymer casing with heat power and convection boundary conditions applied. The resistor is an assembly of two leads and a ceramic casing, with the 1W heat power applied to the inside cavity surfaces in a ratio corresponding to surface area. The free convection is applied to all outside surfaces of the sample assembly. The FEA model is shown in Fig. 4, and the applied boundary conditions are illustrated in Fig. 5. The assembly was meshed with an element size of 1.046 mm and a tolerance 0.052 mm, which resulted in 83,823 total nodes and 59,002 tetrahedral elements.

3.3 Model Calibration

The thermal conductivity of the filled polymer depends on fiber orientation of the filler, which is not necessarily uniform across the sample. Therefore, experimental results from a bulk polyamide sample without filler were first used to validate and calibrate the model. Since the thermal conductivity of the unfilled polymer is isotropic and does not change substantially after injection molding, it ensures uniform heat dissipation and accurate material properties for input into the simulation.

In order to assign adequate material properties to model the embedded surrogate, the resistor was disassembled to determine the materials that were used in its fabrication, as well as their geometries. The casing material was a carbon ceramic measured to be 0.15 mm, while the electrical leads were determined to be copper.

Free convection was applied to all outside surfaces of the sample assembly. However, the resistor leads have two orders of magnitude higher thermal conductivity compared to the other components, and the heat from the embedded resistor dissipates through them more quickly than through the polymer casing. Due to the much smaller area of the leads and their higher temperature, natural convection conditions with different coefficients were applied to the leads and the casing. The values of h were calibrated with experimental data to be 60 and 30 W/m^2-K respectively. The thermal properties of the materials used in the FEA model are listed in Table 3.

Sectioning of the bulk polymer sample showed that the thermocouple was 1.5 mm away from the resistor, due to forces imposed on it while melt injection to the mold. Therefore, the temperature field resulting from the FEA simulation was compared with corresponding experimental data at the thermocouple location. The thermocouple reading was 63.3°C, the corresponding FEA result was 66.9°C and the embedded resistor surface temperature resulting from FEA was 88°C. The cross section temperature field FEA result is shown in Fig. 6**.** Since the maximum error in the FEA prediction was less then 10%, it was determined that the modeling approach was capturing the physics of the thermal conduction process with sufficient accuracy to warrant proceeding to modeling and experimental validation of the thermally conductive filled polymer specimen.

3.4 Modeling of Thermally Conductive Polymer Structures

Since thermal conductivity of the filled polymer depends on fiber orientation of the filler and will not necessarily be uniform across the sample, the modeling approach had to be modified to account for the directionality of the heat conduction that would result from the fiber orientations obtained after the in-mold assembly process. In addition, due to more demanding processing conditions for the filled polymer, voids can potentially develop inside the specimen that must be accounted for in the modeling. Voids (or air traps) are formed when converging flow fronts surround and trap a bubble of air. This is usually caused by racetrack effect, hesitation, unbalanced flow paths or improper venting [15]. Since this work was focused on the practical application of the filled polymers, rather then optimizing the runner system to achieve balanced flow, we tried to model the actual sample as realistically as possible. Therefore, sectioning of the experimental sample was performed by placing it in a milling machine and removing 1 mm thick layer of the material at a time, followed by photographic examination of the cross-section. The photographs revealed the actual void distribution inside the sample, as seen in Fig. 7. This data was then used to introduce simplified voids in the model of the polymer in which the electronic component is embedded. The resulting model with voids is shown on Fig. 8 and was substituted for the previous model to perform the thermal analysis.

After modeling the voids, the fiber orientation had to be accounted for inside the filled polymer specimen. For this purpose, a CFD flow simulation was performed inside the mold using Moldflow Plastics Insight 6.1 to obtain the 3D fiber orientation tensor (degree of orientation). Numerical prediction of the 3D fiber orientation during mold filling in Moldflow is based on an equation of motion for rigid particles in a fluid suspension. The analysis consists of two identifiable terms: (1) the hydrodynamic term [16] and (2) the interaction term [17]. The process simulation settings used are listed in Table 4. The resulting "tensor principal vector as segments" was plotted and scaled to display only the vectors which were aligned more than 75%. These plots were obtained for 5 mm long portions of the cylinder to clarify variation of the results across the axis of the specimen. Sample plots are shown in Fig. 9.

After careful analysis of the above results, it was determined that the cylinder model for the polymer composite could be partitioned into two sub-parts along the length to reflect the directional thermal conductivities based on fiber orientation. These "discretization" approaches have been previously used in modeling processing and performance effects on complex material distributions in composite materials such as Functionally Graded Materials, where the compositions can be continuously varying [18-20].

Due to the directionality of the fibers, the "high" value of k is used along the hoop direction in the bigger partition and along the radial direction in the smaller partition. According to the manufacturer, the thermal conductivity along the perfectly aligned fibers is 11 W/m-K. Given the level of misalignment that was permitted in defining the partitions, the "high" value of k was taken to be 10 W/m-K along the fiber orientation direction. Using a standard rule-of-mixtures formula for transverse and longitudinal conduction relative to the direction of fiber reinforcement for a transverse isotropic material, a value of 1 W/m-K was used in the two other principal directions [21]. The final simplified model is shown in Fig. 10.

Using this model and the same boundary conditions as in the bulk polymer sample, the thermal FEA simulation was performed, and the resulting thermal plot shown in Fig. 11 was compared with experimental data for the filled polymer

sample. The maximum predicted temperature error was found to be less then 11%, therefore verifying that the model approach was sufficiently accurate for thermally conductive filled polymers. The thermocouple reading was 50.5°C, the corresponding FEA result was 45.3°C and the embedded resistor surface temperature resulting from FEA was 51.1°C. These values when compared with the results from the bulk polymer case indicate a significant 40% reduction in the operating temperature of the embedded resistor. Therefore, these results justify the use of thermally conductive filled polymers as the material of choice for embedding actuators. However, one has to keep in mind that a high filler volume fraction responsible for the increased thermal conductivity of the polymer also affects the composite mechanical properties, making the material more brittle. Therefore additional analysis may be needed for structurally critical designs.

3.5 Analysis of Thermal Conductivity for Filled Polymers

After developing a suitably accurate thermal FEA model accounting for the effects of fiber orientation in the filled polymers resulting from the in-mold assembly process, it was possible to predict trends for the thermally conductive, filled polymers. First, the sensitivity of the actual operational temperature and heat dissipation of the embedded component was assessed relative to the directional thermal conductivity resulting from the in-mold assembly process. The model described in Section 3.2 was used with some modifications to the polymer cylindrical casing. Instead of a single part with uniform isotropic properties, it was modeled as an assembly of three cylinders, which combined together to form the original part. Then, different directional values of thermal conductivities were assigned to each of the three cylinders. The modified FEA model is shown in Fig. 12**.** To address the processing conditions, the "high" thermal conductivity direction of the middle part was modeled to be aligned with the injection direction, marked on Fig. 12 with a dotted arrow. For the outer cylinders, the directional thermal conductivity was aligned with the axis of the leads. Then, the values of these thermal conductivities were varied to assess their influence on actual heat dissipation. The variation of the values was done in the following manner: using integer increments, the "high" k (i.e., along the orientation of the fibers) was varied from 4 to 10 W/m-K, while keeping the sum of thermal conductivities in all three principal directions at a constant value of 12. Note, that in the case of k=4, the model had a uniform distribution of k in all directions and represented an isotropic case. With this model, it was possible to predict the maximum surface temperature of the embedded resistor with respect to the fiber orientation. The results of this study are presented in Table 5. The temperature field for the most anisotropic case (principal values 1-1-10/1-10-1) is shown in Fig. 13**.**

It can easily be concluded from Table 5 that the variation of the directional thermal conductivities across the sample does not influence the operating temperature of the embedded heat-generating electronic component in a significant manner, as long as the value of k is high enough. Therefore it was concluded that for this structure with an embedded electronic component, tedious and sophisticated modeling of directional thermal conductivities resulting from manufacturing process can be significantly simplified and reduced, or even omitted.

Next, it was desirable to understand how much can be gained by using polymers with increased thermal conductivity. Therefore based on the previous results, the value of k was varied isotropically and plotted against the predicted surface temperature of the embedded resistor. The resulting plot is shown in Fig. 14**.** From this numerical study, it was concluded that increasing the value of thermal conductivity of the polymer from 0.22 to 2 W/m-K results in a 50% temperature drop of the embedded resistor in operation. However, further increase of k does not substantially decrease the surface temperature of the resistor therefore this value represents an effective "cut-off" for the change in the surface temperature of the resistor with thermal conductivity. This cut-off point can be attributed to free convection in air being the "bottleneck" for heat dissipation. Nevertheless, using thermally conductive polymers shows significantly improved heat dissipation and promising use of these materials as multi-functional anchoring structures to facilitate miniaturization of devices.

4 Incorporating In-mold Assembly Process Constraints during the Optimization

The mold used for in-mold assembly, in addition to all regular mold designing rules, needs to be designed in a way to allow for fixating actuators in order for them to be embedded correctly. This also requires securing heat sensitive features of the actuators from the hot polymer melt. During injection molding, the high-pressure polymer melt being injected into the mold cavity has the potential to destroy delicate features of the actuator before it is fully embedded, which may prevent

the actuator from functioning properly. The injection temperature and pressure are the most important parameters to be controlled, ensuring both proper filling of the mold and survivability of the embedded actuator.

To demonstrate the feasibility of embedding actuators using the in-mold assembly process, a case of an actuator anchored in a polymer structure was studied. A simple motor holder was designed to reveal the difference in heat dissipation when the actuator is placed in a thermally conductive polymer versus a bulk polymer structure. The same polymers were used as in the experiment described in Section 3.1, while a Didel SS 7 mm blue pager motor producing a maximum of 1.5 W was used as the power input. The structure was designed for a 12-teeth pinion on the motor shaft to be engaged with a 60-teeth spur gear on the output shaft. The output shaft was placed in an in-mold assembled brass sleeve to minimize friction.

Initial experiments indicated that the steel motor housing was being permanently deformed while injecting the polymer into the mold cavity. This survivability issue had to be addressed by determination of correct size of the embedding structure and the packing pressure during injection. Reduction of the part thickness will reduce the area of the compressive pressure being exerted on the actuator. However it is constrained in this case by the tooling available for manufacturing the molds. On the other hand, reduction of packing pressure may lead to incomplete filling of the mold. Therefore a numerical model of the motor casing and the pressure applied during polymer melt was developed using ANSYS 11.0 FEA software to quantify this interaction and determine the injection pressure needed for successful in-mold assembly of the actuator without preventing proper functioning of the actuator. The motor housing was modeled as a series of cylinders to reflect the actual part and applied boundary conditions. The housing thickness was measured to be 0.4 mm and modeled accordingly. Measurements of the motor coil inside the housing determined the clearance between these elements to be 0.25 mm in the radial direction. It was assumed that the actual deformation should not exceed 1/3rd of the clearance value to practically ensure the functionality of in-mold assembled part.

The ANSYS model was meshed with SOLID92 elements, and material properties for steel were used for the metal housing (Young's Modulus of 200 MPa and Poisson's ratio of 0.27). The boundary conditions applied were zero-displacement of the cylindrical part of the housing tightly constrained by the mold cavity and a pressure applied to the neighboring cylindrical segment, which was exposed to the injection pressure during the in-mold assembly process. Figure 15 shows the part dimensions and a schematic of the applied boundary conditions.

As a result of the ANSYS FEA, the acceptable pressure applied to the motor housing during the in-mold assembly process was determined to be 5.59 MPa, which resulted in a permanent deformation of 0.087 mm that was within the acceptable range. Moldflow simulations were performed to ensure this value will result in complete mold filling.

After determining the appropriate injection pressure to maintain actuator functionality, motor holders were manufactured using the in-mold assembly process. The in-mold assembly mold setup is shown in Fig. 16 and the successfully in-mold assembled parts are shown in Fig. 17. The injection parameters used for the in-mold assembly process are listed in Table 6.

For the heat dissipation experiment, a load was applied to the motor shaft to generate maximum power. With careful control of the voltage supplied to the motor and the current drawn, it was possible to maintain a constant power of 1.5 W. An Omega® 5TC-GG-K-20-36 thermocouple was used to measure the surface temperature of the embedded DC motors. The results of the experiment are listed in Table 7**.** The thermal studies were modeled using the approach described in Section 3 except for the following:

1) a different geometry was used for the encasing polymer;

2) the resistor was replaced with the pager motor assembly;

3) there was no void structure around the motor assembly.

For the unfilled polymer sample, the FEA prediction of the embedded motor temperature was 102°C, which was 6% more than the measured value. For the filled Nylon 12 sample, where thermal conductivity was modeled to be 4 W/m-K in all principal directions, the FEA result was 68.9°C, which was 5% more than the measured value. The accuracy of these results were consistent with the previous experimental and numerical comparisons. Thus, this case study clearly shows that embedding the DC pager motor in a thermally conductive filled polymer results in reduction of its working temperature by 46% when compared to the bulk polymer casing. This further proves the concept that thermally conductive polymers are more effective in terms of heat dissipation, and hence are the material of choice for building multi-functional structures with embedded actuators. The modeling approach was also established for enabling feasible design of embedded actuators using the in-mold assembly process.

5 Conclusions

This paper describes a systematic approach for designing multi-functional, filled polymer structures with embedded actuators using in-mold assembly process to facilitate the miniaturization of devices. The novel aspects of this work include: (1) determination of effective thermal conductivity of filled polymer composites for heat dissipation task and (2) determination of design and processing conditions to ensure survivability of the embedded actuator using in-mold assembly process through concurrent optimization of choice of material, size of the structure and processing conditions.

The method described in this paper is applicable to any multi-functional structure with embedded actuators that can be manufactured using filled polymers and in-mold assembly process. We have described an integrated design methodology for these structures taking into account: (1) selection of a moldable material for ensuring thermal performance, (2) a mold design for successfully realizing in-mold assembly, (3) influence of gate placement on thermal performance, and (4) influence of processing conditions on survivability of the embedded actuator. The following new results are reported in this paper. First, we present an integrated thermal modeling methodology for designing multi-functional structures using filled polymers under functionality and moldability constraints. Second, we use this methodology to assess effective thermal conductivity of filled polymers for the heat dissipation task. Next, we determine the influence of the fiber orientation on the functionality of filled polymer structures for embedding actuators. Finally, we describe an approach for determining processing conditions resulting in successful in-mold assembly of embedded actuators.

Our design framework was experimentally verified to be sufficiently accurate for predicting thermal behavior of filled polymer multi-functional structures. The use of these thermally conductive polymers resulted in significant improvement in dissipation of heat from actuators embedded in the structure when compared to unfilled polymers. The influence of gate placement was determined to be of minor significance on the heat-dissipation task. Once a critical level of thermal conductivity of the polymer is reached, there exist a heat-transfer path and natural free convection becomes the bottleneck for the dissipation of heat from embedded actuator. Therefore we have shown that tedious and computationally-expensive modeling of fiber orientation resulting from process design is not necessary from the thermal management point of view, as long as thermal conductivity of the polymer exceeds 2 W/m-K. Successful in-mold assembly of an example multi-functional structure consisting or an actuator embedded in a motor holder assembly was obtained through optimal design of the structure and processing conditions for the choice of filled polymer. Therefore, we have been able to demonstrate the feasibility of designing multi-functional structures from filled polymers by embedding actuators using in-mold assembly to facilitate the miniaturization of devices.

6 Acknowledgements

This work was supported by NSF grants EEC0315425 and DMI0457058, and by ONR award number N000140710391. Opinions in this paper are those of the authors and do not necessarily reflect those of the sponsors.

7 References

[1] Kim, K. J., and Tadokoro, S., 2007, "Electroactive Polymers for Robotic Applications, " Springer,

[2] Rosmarin, J. B., and Asada, H. H., 2008, "Synergistic Design of a Humanoid Hand with Hybrid DC Motor – SMA Array Actuators Embedded in the Palm," Proceedings of the IEEE International Conference on Robotics and Automation, Pasadena, CA, pp. 773-778.

[3] Pappafotis, N., Bejgerowski, W., Gullapalli, R., Simard, J. M., Gupta, S. K., and Desai, J. P., 2008, "Towards Design and Fabrication of a Miniature MRI-Compatible Robot for Applications in Neurosurgery," Proceedings of the ASME 2008 IDETC/CIE, New York, NY.

[4] Bejgerowski, W., Ananthanarayanan, A., Mueller, D., and Gupta, S. K., 2009, "Integrated Product and Process Design for a Flapping Wing Drive-Mechanism," Journal of Mechanical Design, **131**, No.6, pp. 061006.

[5] Wood R.J., Avadhanula, S., Sahai, R., Steltz, E., and Fearing R.S., 2008, "Microrobot Design Using Fiber Reinforced Composites," Journal of Mechanical Design, **130**, No.5, pp.052304.

[6] Crippa G., Davoli P., 1995, "Comparative Fatigue Resistance of Fiber Reinforced Nylon 6 Gears," Journal of Mechanical Design, **117**, No.1, pp.193.

[7] Weber, E. H., Clingerman, M. L., and King, J. A., 2002, "Thermally Conductive Nylon 6,6 and Polycarbonate Based Resins. I. Synergistic Effects of Carbon Fillers," J. App. Polymer Sc., **88**, No.1, pp. 112-122.

[8] Bahadur, R., and Bar-Cohen, A., 2005, "Thermal Performance Limits of Polymer Composite Pin Fin Heat Sinks," Proceedings of the 55th Electronic Components and Technology Conference, **2**, pp. 1720-1727.

[9] Bahadur, R., 2005, "Characterization, Modeling and Optimization of Polymer Composite Pin Fins," Ph.D. Thesis, Mechanical Engineering Department, University of Maryland, College Park, MD.

[10] Dogruoz, M. B., and Arik, M., 2008, "An Investigation on the Conduction and Convection Heat Transfer from Advanced Heat Sinks," Proceedings of the 11th Intersociety Conference on Thermal and Thermomechanical Phenomena in Electronic Systems, Orlando, FL, pp. 367-373.

[11] Egelkraut, S., Heinle, C., Eckardt, B., Kramer, P., Brocka, Z., Marz, M., Ryssel, H., and Ehrenstein, G. W., 2008, "Highly Filled Polymers for Power Passives Packaging," Proceedings of the 2nd Electronics System Integration Technology Conference, London, UK, pp. 403-410.

[12] Alawadhi, E. M., and Amon, C. H., 2003, "PCM Thermal Control Unit for Portable Electronic Devices: Experimental and Numerical Studies," IEEE Transactions on Components and Packaging Technologies, **26**, No.1, pp. 116-125.

[13] Egan, E., and Amon, C. H., 2001, "Measuring Thermal Conductivity Enhancement of Polymer Composites: Application to Embedded Electronics Thermal Design," J. Enhanced Heat Transfer, **8**, No.2, pp. 119-135.

[14] Goldstein, R. J., Eckert, E. R. G., Ibele, W. E., Patankar, S. V., Simon, T. W., Kuehn, T. H., Strykowski, P. J., Tamma, K. K., Heberlein, J. V. R., Davidson, J. H., Bischof, J., Kulacki, F. A., Kortshagen, U., and Garrick, S., 2003, "Heat Transfer - a Review of 2001 Literature," Int. J. Heat and Mass Transfer, **46**, No.11, pp. 1887-1992.

[15] Shoemaker, J., 2005, "Moldflow Design Guide: A Resource for Plastics Engineers, " Hanser Publishers, Munich.

[16] Jeffery, G. B., 1922, "The Motion of Ellipsoidal Particles Immersed in Viscous Fluid," Proceedings of the Royal Society of London, **A102**, pp. 161.

[17] Folgar, F. P., and Tucker, C. L., 1984, "Orientation Behavior of Fibers in Concentrated Suspensions," Reinforced Plastic Composites, **3**, No.2, pp. 98-119.

[18] Bruck, H. A., 2000, "A One-Dimensional Model for Designing Functionally Graded Materials to Attenuate Stress Waves," Int. J. Solids and Structures, **37**, pp. 6383-6395.

[19] Rabin, B. H., Williamson, R. L., Bruck, H. A., Wang, X.-L., Watkins, T. R., and Clarke, D. R., 1998, "Residual Strains in an Al_2O_3-Ni Joint Bonded with a Composite Interlayer: Experimental Measurements and FEM Analysis," J. American Ceramic Society, **81**, pp. 1541-1549.

[20] Shabana, Y. M., Pines, M. L., and Bruck, H. A., 2006, "Modeling the Evolution of Stress Due to Differential Shrinkage in Powder-Processed Functionally Graded Metal-Ceramic Composites During Pressureless Sintering," Int. J. Solids and Structures, **43**, pp. 7852-7868.

[21] Paul, B., 1960, "Prediction of Elastic Constants of Multiphase Materials", Transactions of the Metallurgical Society of AIME, **218**, pp. 36-41.

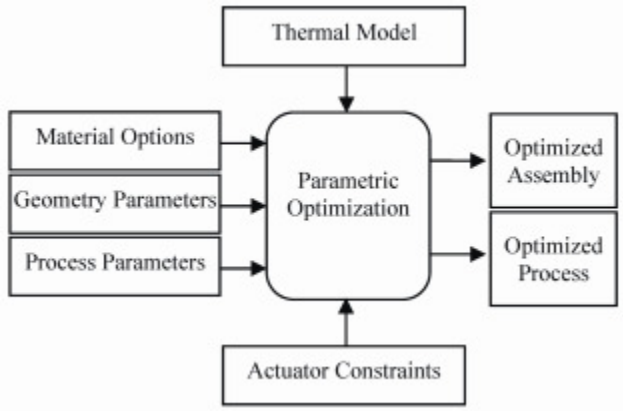

Fig. 1 Parametric optimization of in-mold assembly using thermally conductive polymers

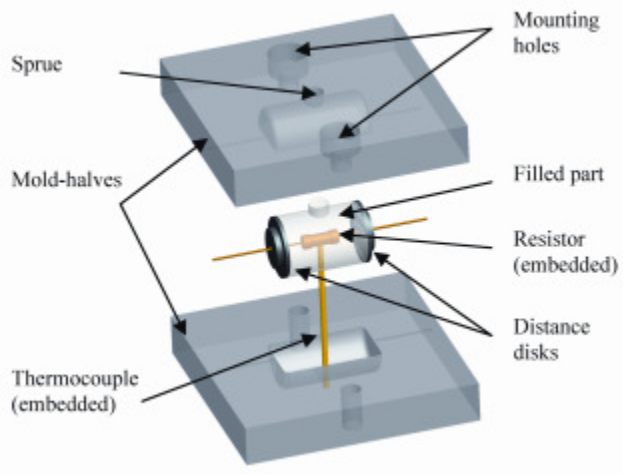

Fig. 2 Embedded resistor: in-mold assembly

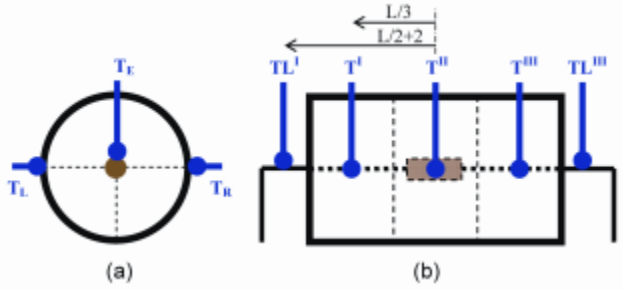

Fig. 3 Temperature sampling points: (a) cross-section and (b) side view

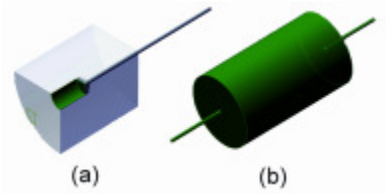

Fig. 4 FEA model assembly: (a) leads (b) ceramic casing (c) polymer casing

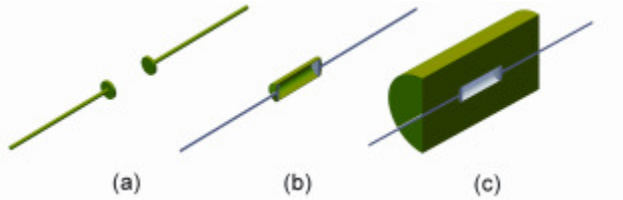

Fig. 5 Surfaces for applying FEA boundary conditions (in green): (a) heat power, (b) convection to air

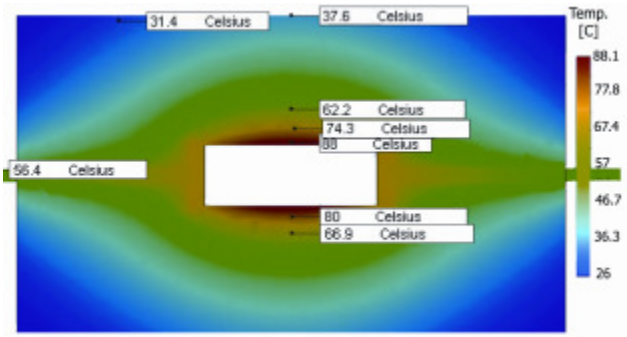

Fig. 6 Temperature field FEA result for unfilled Nylon 12 sample

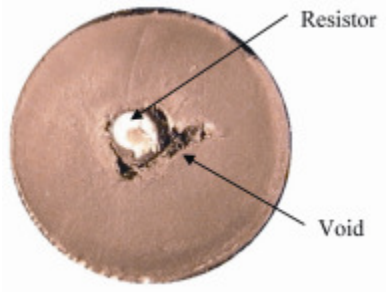

Fig. 7 Cross-sectioning of the embedded resistor specimen

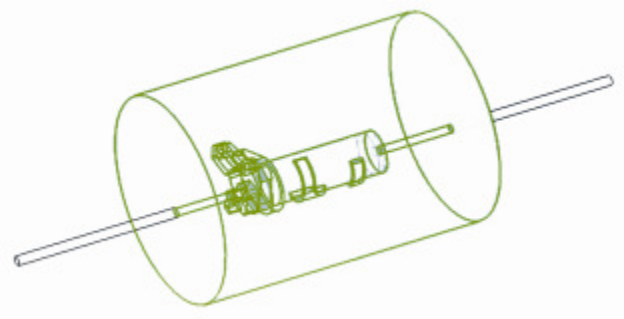

Fig. 8 FEM model with voids

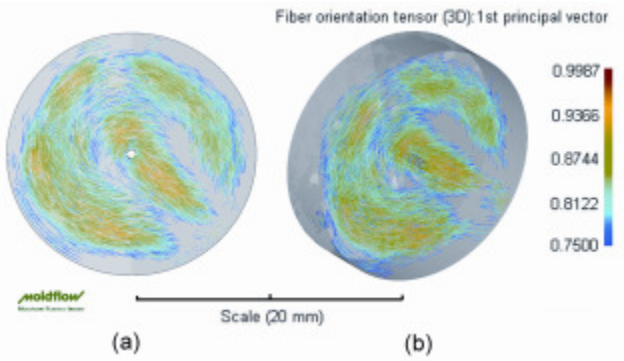

Fig. 9 Mold flow simulation sample result: (a) side view and (b) isometric view of a segment

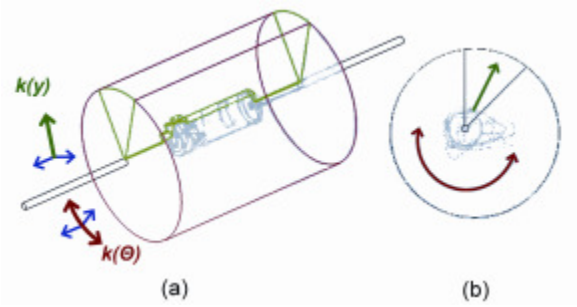

Fig. 10 FEM model with orthotropic thermal conductivities assigned: (a) isometric view and (b) side view

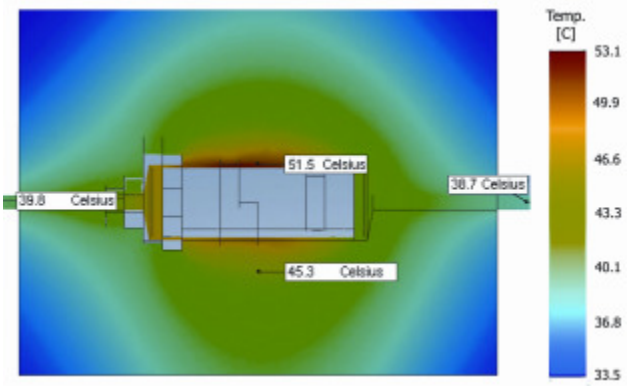

Fig. 11 Temperature field FEA result for NJ-6000 TC filled polymer composite

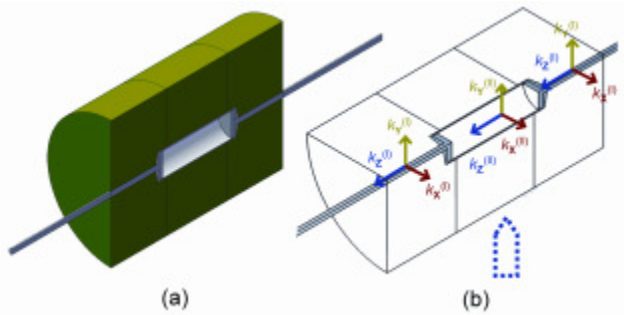

Fig. 12 Modified FEA model: (a) assembly, (b) directional thermal conductivities

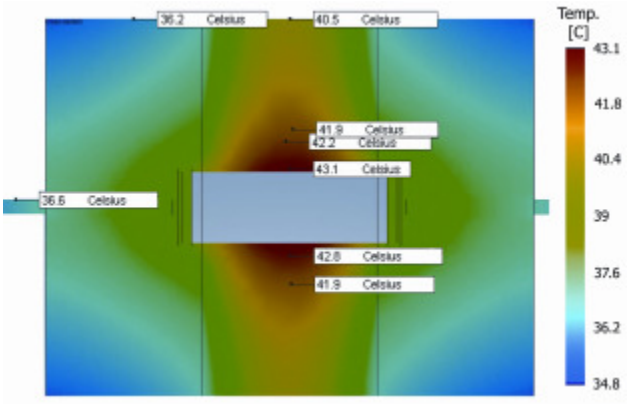

Fig. 13 Temperature field FEA result for the most anisotropic case (1-1-10/1-10-1)

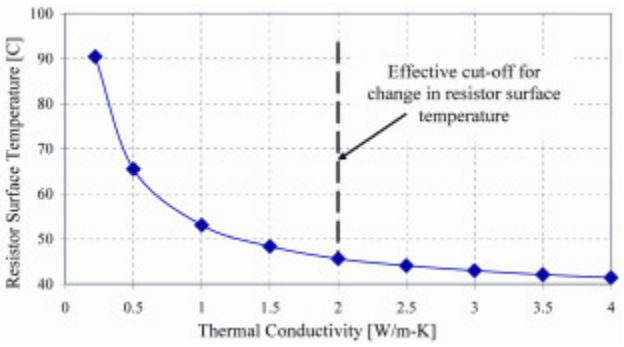

Fig. 14 Isotropic thermal conductivity influence on the temperature of embedded component

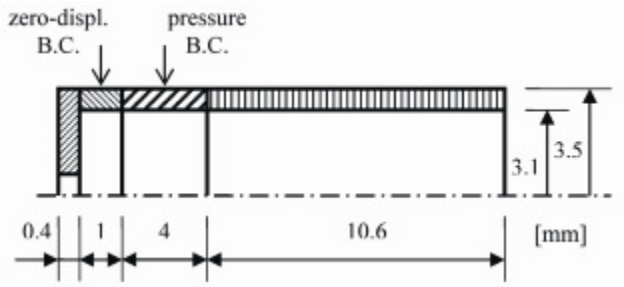

Fig. 15 ANSYS model key dimensions and boundary conditions

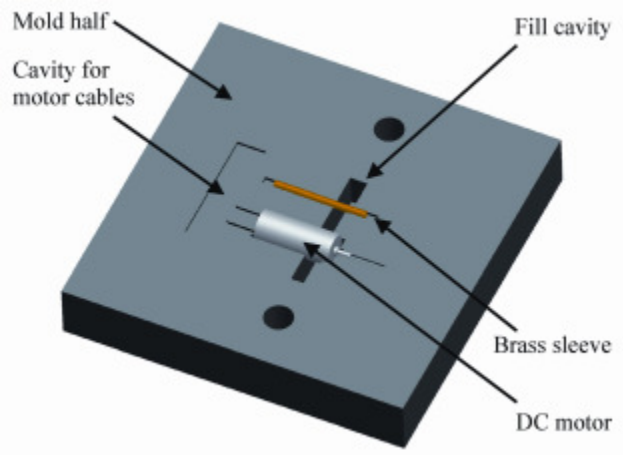

Fig. 16 In-mold assembly setup for manufacturing the motor holder

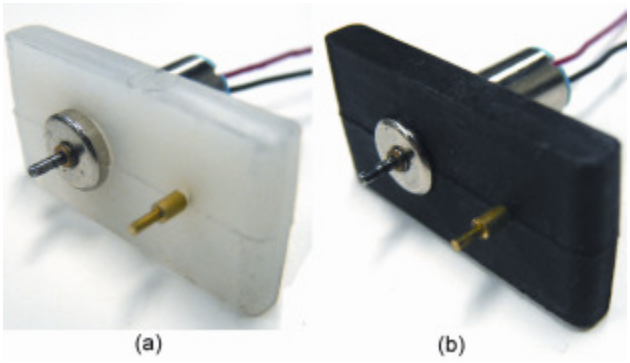

Fig. 17 In-mold assembled motor holders: (a) unfilled Nylon 12, (b) thermally conductive filled Nylon 12

Table 1 Properties of materials used in the experiment [based on manufacturer's datasheets]

Measure	Unit	Grilamid L16	NJ-6000 TC	Test Method
Density	*kg/m*	1010	1610	ASTM D792
Thermal Conductivity	*W/m-K*	0.22	11	ASTM C177
Tensile Strength	*MPa*	42	110	ASTM D638
Elongation at Break	*%*	275	1.9	ASTM D638
Flexural Modulus	*GPa*	1.3	22.2	ASTM D790
Flexural Strength	*MPa*	59	109	ASTM D790
Volume Resistivity	*Ohm-cm*	10^{14}	10^{2} to 10^{3}	ASTM D257
Melt Temperature	*°C*	190 to 270	260 to 277	

Table 2 Sample dimensions

Parameter	Symbol	Unit	Grilamid L16	NJ-6000 TC
Resistor radius	r_1	*m*	1.91E-03	1.91E-03
Cylinder radius	r_2	*m*	9.27E-03	9.27E-03
Cylinder length	*L*	*m*	3.18E-02	2.54E-02

Table 3 Thermal properties used in FEA

Material	Thermal conductivity [W/m-K]	Mass density [kg/m^3]
Resistor copper leads	230	8400
Resistor carbon ceramic casing	15	2300
Grilamid L16	0.22	1010
NJ-6000TC	11	1610

Table 4 Process settings used in flow simulation

Parameter	Value
Injection material	POLYONE NJ-6000 TC Black
Fibers/fillers	51.8% Cytec DKD Filled
Injection temperature	270 C
Mold temperature	35 C
Injection velocity	6.2 cc/s
Mold-open time	5 s

Table 5 Temperature [C] of embedded resistor as a function of different directional thermal conductivities

k^I k^{II}	**1-10-1**	**2-8-2**	**3-6-3**	**4-4-4**
1-1-10	43.5	41.5	40.9	40.9
2-2-8	43.1	41.2	40.6	40.7
3-3-6	43.0	41.2	40.6	40.7
4-4-4	43.2	41.4	40.8	40.8

Table 6 In-mold assembly process parameters

Parameter	Value
Packing pressure	5.59 MPa
Cycle time	2.7 s
Injection time	0.4 s
Injection temperature	195 C (Grilamid L16) 270 C (NJ-6000TC)
Mold temperature	35 C

Table 7 Results of the embedded motor experiment

Parameter	Unit	Unembedded	Nylon 12	NJ-6000 TC
Voltage	*V*	3.00	3.00	3.00
Current	*A*	0.5	0.5	0.5
Temperature	*C*	120.2	96.0	65.5